

Contents lists available at [ScienceDirect](http://ScienceDirect)

# Quaternary Science Reviews

journal homepage: [www.elsevier.com/locate/quascirev](http://www.elsevier.com/locate/quascirev)

## A long-term context (931–2005 C.E.) for rapid warming over Central Asia



N.K. Davi<sup>a, b, \*</sup>, R. D'Arrigo<sup>a</sup>, G.C. Jacoby<sup>a</sup>, E.R. Cook<sup>a</sup>, K. Anchukaitis<sup>c</sup>, B. Nachin<sup>d</sup>,  
M.P. Rao<sup>a, e</sup>, C. Leland<sup>a, e</sup>

<sup>a</sup> Tree-Ring Laboratory, Lamont-Doherty Earth Observatory, 61 Route 9W Palisades, New York, 10964, USA

<sup>b</sup> Department of Environmental Science, William Paterson University, Wayne, NJ, 07470, USA

<sup>c</sup> Dept. of Geology and Geophysics, Woods Hole Oceanographic Institute, Woods Hole, MA, 02543, USA

<sup>d</sup> Department of Forestry, National University of Mongolia, Ulaanbaatar, 14201, Mongolia

<sup>e</sup> Department of Earth and Environmental Science, Columbia University in the City of New York, NY, 10027, USA

### ARTICLE INFO

#### Article history:

Received 19 November 2014

Received in revised form

27 April 2015

Accepted 16 May 2015

Available online

#### Keywords:

Paleoclimate

Temperature

Tree-ring

Mongolia

Reconstruction

Dendrochronology

Global warming

### ABSTRACT

Warming over Mongolia and Central Asia has been unusually rapid over the past few decades, particularly in the summer, with surface temperature anomalies higher than for much of the globe. With few temperature station records available in this remote region prior to the 1950s, paleoclimatic data must be used to understand annual-to-centennial scale climate variability, local response to large-scale forcing mechanisms, and the significance of major features of the past millennium such as the Medieval Climate Anomaly (MCA) and Little Ice Age (LIA) both of which can vary globally. Here we use an extensive collection of living and subfossil wood samples from temperature-sensitive trees to produce a millennial-length, validated reconstruction of summer temperatures for Mongolia and Central Asia from 931 to 2005 CE. This tree-ring reconstruction shows general agreement with the MCA (warming) and LIA (cooling) trends, a significant volcanic signature, and warming in the 20th and 21st Century. Recent warming (2000–2005) exceeds that from any other time and is concurrent with, and likely exacerbated, the impact of extreme drought (1999–2002) that resulted in massive livestock loss across Mongolia.

© 2015 Elsevier Ltd. All rights reserved.

### 1. Introduction

Our understanding of long-term temperature variability and its causes is extremely limited in remote Central Asia, due to short and sparse meteorological data, as well as a paucity of long-term, high-resolution, temperature-sensitive proxy records. Instrumental records, typically only reaching back to the 1940s or later, show that temperatures in Central Asia have been increasing rapidly, particularly since the mid 1990's, and are currently warmer than any other time in recorded history (Chen et al., 2009). Paleoclimate reconstructions, largely derived from tree-ring records, have been used to extend our understanding of temperature across Mongolia and Central Asia (Jacoby et al., 1996; D'Arrigo et al., 2000; D'Arrigo et al., 2001a;; Myglan et al., 2012) on long-term scales. Among the existing temperature tree-ring records from Central Asia, few

extend back to the early Medieval Climate Anomaly (MCA, ca. 850–1050 C.; Lamb, 1965; see Cook et al., 2013). The only regional chronology thus far, from *Solongotyn Davaa*, in Mongolia's central Tarvagatay Mountains, extends back to 262 C.E., based on living and subfossil wood of Siberian pine (D'Arrigo et al., 2001a). However, this long record could not be used to generate calibrated and validated reconstructions, due to the limits of nearby meteorological station records. These cover only a few decades, are situated at lower elevations, and are quite distant from the tree-ring sites.

Here, we develop a millennium-length (931–2005 C.E.) tree-ring chronology from Siberian larch trees (*Larix sibirica*) growing at elevational treeline sites in Mongolia, where the dominant limiting factor for growth is temperature (Jacoby et al., 1996; D'Arrigo et al., 2000, 2001a, b). The chronology and reconstruction, from a site named *Ondor Zuun Nuruu* (OZN; meaning 'High East Ridge'), has an unusually large sample depth (>200 samples) and can be calibrated and validated using regionalized meteorological data from Mongolia and Russia. The reconstruction allows us to evaluate temperature variability and extremes over the past

\* Corresponding author. Department of Environmental Science, William Paterson University, Wayne, NJ, 07470, USA.

E-mail address: [ndavi@ldeo.columbia.edu](mailto:ndavi@ldeo.columbia.edu) (N.K. Davi).

millennium in Central Asia, a region that is warming faster than many places on Earth (Chen et al., 2009). It also places recent warming trends into a long-term context, contributes to our understanding of spatial patterns of the MCA and LIA, and provides evidence of significant volcanic influence on Central Asia temperature.

## 2. Materials and methods

### 2.1. Instrumental data

The OZN tree-ring site is located just west of Lake Hovsgol, in north central Mongolia near elevational treeline (2400 m, Fig. 1),

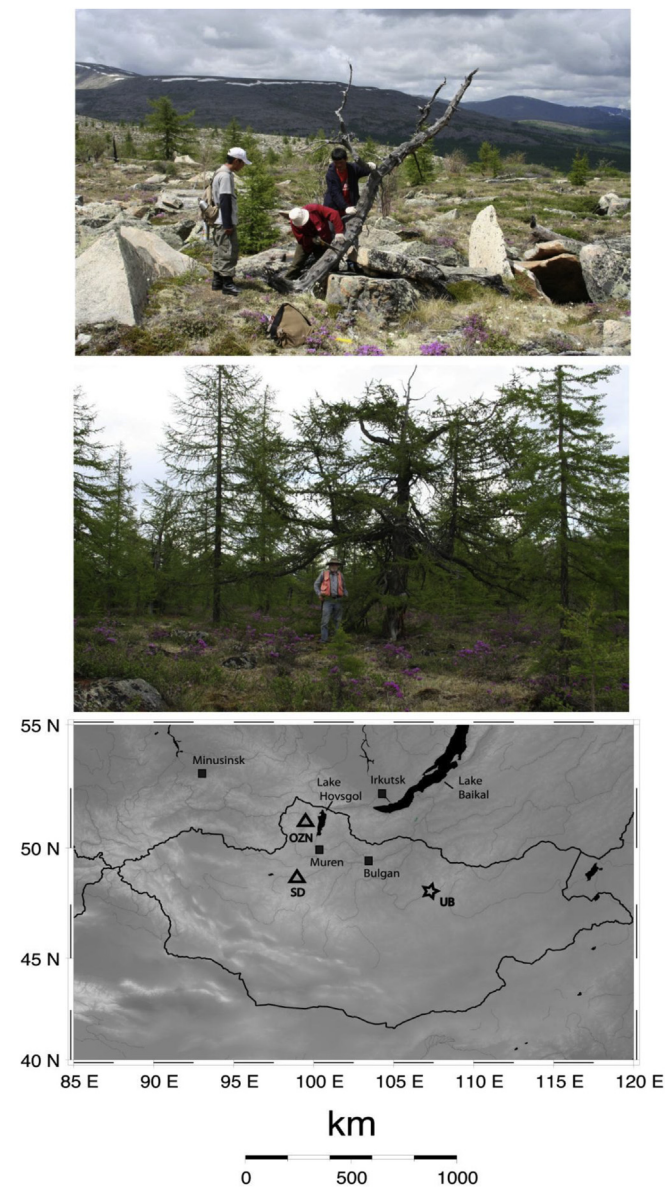


**Fig. 1.** Top: Students sampling a relict tree at upper treeline at the Ondor Zuun Nuruu site. Middle: An example of a long-lived Siberian Larch tree at Ondor Zuun Nuruu. Bottom: Map showing the location of Ondor Zuun Nuruu and Solongotyn Davaa sites (triangles), the four meteorological stations (squares), and the capital of Mongolia Ulaanbaatar (star). Greyscale shows elevation with higher areas in lighter colors. Lakes are labeled and shaded in black. The Rinchinlhumbe station is located within the OZN triangle. (For interpretation of the references to colour in this figure legend, the reader is referred to the web version of this article.)

and is in one of the coldest regions in Central Asia. Instrumental temperatures from Rinchinlhumbe (Table 1), the nearest station to the OZN site (~50 km away), average  $-29^{\circ}\text{C}$  in winter (DJF), and  $12^{\circ}\text{C}$  in the summer (JJA), typical of the extreme continentality of Central Asia. We estimate that temperatures at the OZN site are between  $-6^{\circ}\text{C}$  and  $-9^{\circ}\text{C}$  colder than the Rinchinlhumbe site (~900 m lower) based on adiabatic lapse rates. The nearest and most complete precipitation station record comes from Muren (~143 km from OZN) (Table 1). Total annual (Jan–Dec.) precipitation for Muren from 1941 to 2014 is 221 mm with the majority of that precipitation (167 mm) falling in June, July and August.

There are few long temperature records from this region. The Rinchinlhumbe station which is closest to our site has a temperature record that begins only in 1974. To the north of OZN in Russia, station records reach as far back as the late 1800 s at Minusinsk and into the 1830 s at Irkutsk (Fig. 1, Table 1). In Mongolia, the nearest and most complete station records are for Bulgan and Muren (1941–2011), both relatively high elevation sites (>1200 m), and more similar to the higher elevation OZN treeline site. We thus generated a regional temperature record by averaging the data from Irkutsk, Minusinsk, Muren and Bulgan. Average June–July temperatures from Mongolia (Bulgan & Muren), and Russia (Irkutsk & Minusinsk) correlate at  $r = 0.5$  ( $p < 0.05$ ) over the 1941–2005 period. There were a total of nine missing values in the four station records and each was replaced with the corresponding monthly average. Gridded temperature data from the Climate Research Unit (CRU TS 3.10, Harris et al., 2014) was also evaluated in order to compute spatial correlations of temperature with the reconstruction.

### 2.2. Tree-ring data

The OZN tree-ring site is located near the upper forest border near elevational treeline (2400 m) on a west-facing slope of large granite slabs with pockets of soil, abundant moisture, and shallow or perched water table. Larch trees grow primarily on soil “islands” amidst the granite-boulder talus. Similar to Sol Dav (D’Arrigo et al., 2001a), OZN is an open canopy site and alpine shrubs and grasses grow near the trees, an indication of mesic conditions. Elevation, proximity to treeline and microsite features all indicate that temperature is likely to be the primary factor limiting tree growth at OZN. These trees are extremely slow-growing and long-lived. One living tree dated back to 1405 and had a diameter of roughly 36 cm (an average annual growth rate of only ~0.3 mm per year). The oldest living tree dated back to 1374. There were also abundant relict logs scattered throughout the site. All living trees were sampled non-destructively by coring, and cross-sections or cores were taken from dead trees. Sample depth at this site is substantial, with a total of 209 samples collected, over half (133) coming from subfossil wood.

Ring-width series were detrended using Signal Free (SF) and Regional Curve Standardization (RCS) procedures (Melvin and Briffa, 2008), which aid in the preservation of long-term, centennial scale variability in excess of the segment lengths of the

**Table 1**  
Meteorological station coordinates, elevation and time-span.

	Coordinates	Elevation	Span
Irkutsk <sup>a</sup>	52.27N, 104.32E	469 m	1820–2011
Muren <sup>a</sup>	49.57N, 100.17E	1283 m	1941–2011
Bulgan <sup>a</sup>	48.80N, 103.55E	1208 m	1941–2011
Minusinsk <sup>a</sup>	53.70N, 91.70E	254 m	1886–2011
Rinchinlhumbe	51.12N, 99.67E	1583 m	1974–2011

<sup>a</sup> Used for modeling.

individual tree-ring series being processed (Cook et al., 1995). We use the program RCSigFree created by E. R. Cook, P. J. Krusic and T. Melvin (<https://www.ldeo.columbia.edu/tree-ring-laboratory/resources/software>). Prior to SF-RCS detrending, adaptive power transformations were applied to the ring-width measurements (Cook and Peters, 1997). Doing so stabilizes the variance of the ring-width series and protects the resulting detrended indices from potential inflationary bias, especially at the outer end of the chronology. See Cook and Peters (1997) for details. The RCS curve itself was estimated by aligning and averaging all tree-ring data by biological age and fitting a smooth time-varying spline to the average (Melvin et al., 2007). The resulting smoothed RCS curve was then used to detrend each individual power-transformed ring-width series and the residuals were averaged into a mean chronology after the data were re-aligned to their original calendar years. In the iterative signal free version of RCS used here, the final SF-RCS chronology converged after 3 iterations, after which there was no meaningful change in the SF-RCS chronology. See Melvin and Briffa (2013) for procedural details of the method.

The resulting SF-RCS chronology spans from 715 to 2005 CE, with a mean segment length of 348 years for all series. We truncated the chronology at the year 931, when sample depth drops below six series and three trees. The Expressed Population Signal (EPS; Cook and Kairiukstis, 1990) measures the strength of the common signal for a set of tree-ring series in a given chronology. EPS remains at 0.84 or above throughout the period 931–2005. Generally a level of 0.85 or above is considered a common but arbitrary threshold (Wigley et al., 1984), although should not be interpreted rigidly. RBAR, the mean correlation between tree-ring series, a measure of common variance or signal strength, ranged from 0.37 to 0.73, with a mean of 0.49.

### 2.3. Superposed epoch analysis

We investigated the presence of a volcanic cooling signal in the OZN reconstruction using Superposed Epoch Analysis (SEA, Haurwitz and Brier, 1981). Two methods of significance testing – random sampling and block reshuffling, were used to assess statistical significance given the presence of tree-ring autocorrelation (Adams et al., 2003). Ring width indices in particular can have a significant year-to-year autocorrelation due to persistent biological influences following growing season conditions (D'Arrigo et al., 2013), which can affect the detection of volcanic signals in tree rings. In both cases, the number of Monte Carlo iterations applied was 10,000. The SEA is performed by normalizing the data by the mean of the pre-event years by subtracting, from each event window temperature series, the average of the values for the years–before–the event corresponding to that window (see Fischer et al., 2007). We generated two different large tropical volcanic event year lists using estimates of global volcanic forcing during the last millennium, from Gao et al. (2008) (1177 1214 1259 1276 1285 1342 1453 1601 1642 1763 1810 1816 1836 1992) and Crowley et al. (2008) (1229 1258 1286 1456 1600 1641 1695 1809 1815 1884 1992), because of uncertainty in the timing and magnitude of past explosive volcanism (Schmidt et al., 2012). We created these event year lists by querying the global forcing series for years with negative forcing of at least the magnitude of the Pinatubo (1991) eruption, and then using only the first year if there were multiple consecutive years with large negative forcing (i.e. for 1258, this means using 1258 from the Crowley et al. (2008) data and not 1259 and 1260). We note that Krakatoa is missing from the Gao et al. (2008) event list because it is smaller in magnitude ( $-1.63 \text{ w/m}^2$ ) than Pinatubo ( $-2.48 \text{ w/m}^2$ ) in the global annual compilation from Schmidt et al. (2012), and therefore didn't meet our a priori criteria. Large extratropical Northern Hemisphere eruptions,

such as Laki in 1783 and Katmai in 1912, are not associated with global-scale forcing but can influence Central Asian summer temperatures and these events are examined separately.

## 3. Results

Correlation coefficients were calculated between the OZN chronology and monthly instrumental temperature records for the region (Fig. 2). Temperature was always positively correlated with tree growth indicating that warmer temperatures enhanced growth. Since the strongest positive correlations were consistently found with current June ( $r = 0.62$ ,  $p < 0.01$ ) and July ( $0.43$ ,  $p < 0.01$ ) temperatures, we averaged June and July values from the four nearest and most complete stations as described above (Table 1). As expected, based on site characteristics, we did not find any significant correlation between tree growth and precipitation using the Muren station precipitation data.

We used the SF-RCS chronology as the predictor and the regionalized station temperature data as the predictand in a principal component regression (Cook et al., 1994) to produce a summer temperature reconstruction for the past 1075 years. To evaluate the fidelity of the model a split calibration/validation method was used on both the 1941–1973 and 1974–2005 periods. The reconstruction has significant skill, based on the Reduction of Error (RE), and Coefficient of Efficiency (CE) statistics (Cook and Kairiukstis, 1990) (Table 2). The reconstruction explains 43% of the variance in the instrumental series and captures the year-to-year variations in the regionalized station data over the common period (Fig. 3a). A model based on longer records from Russia alone (1886–2011) did not validate and neither did validation on the Russian records using early 20th Century data (1910–1940). This result is not surprising considering the considerable distance between the OZN site and the Russian stations, and their differences in elevation, illustrating the difficulty in creating and need for high-resolution proxies such as tree rings in such remote regions. Despite their distance to the OZN site the Russian stations improve the model. Without the Russian meteorological data the model explains 38% of the variance compared to 43% with the Russian data.

A comparison of the OZN temperature reconstruction with CRU gridded summer temperatures (Fig. 4) reveals the spatial extent of the relationship between tree growth and temperature – significant correlations cover a sizeable area of Central Asia ( $p < 0.1$ ). We also tested the model by averaging gridded CRU TS3.10 data from 95 to 105°E and from 47 to 53°N. Results were similar (variance explained = 41%,  $p < 0.01$ ), but slightly lower than the model based on the averaged station data (variance explained = 43%,  $p < 0.01$ ). We did not test the earlier portion of the gridded data (1901–1940) because the underlying station data that is used to develop the gridded CRU data is extremely sparse during this time.

## 4. Discussion

### 4.1. Variability through time

The reconstruction reveals considerable variability through time on annual to multidecadal and longer time scales (Fig. 3b), including sustained warm and cold episodes that broadly coincide with the MCA and LIA epochs as described elsewhere for this region (Cook et al., 2013). Reconstructed summer temperatures range from 12.8 to 19.2 °C. The coldest, sustained multi-decadal epoch occurred in the 900s when temperatures remained below the long-term mean (15.8 °C) for 50 years from 934 to 984 (Fig. 3b). This severe cold period was followed by rapid warming from 996 to 1015 and again from 1074 to 1093. These latter periods are the 3rd and 6th warmest 20-year periods (respectively) in the entire record

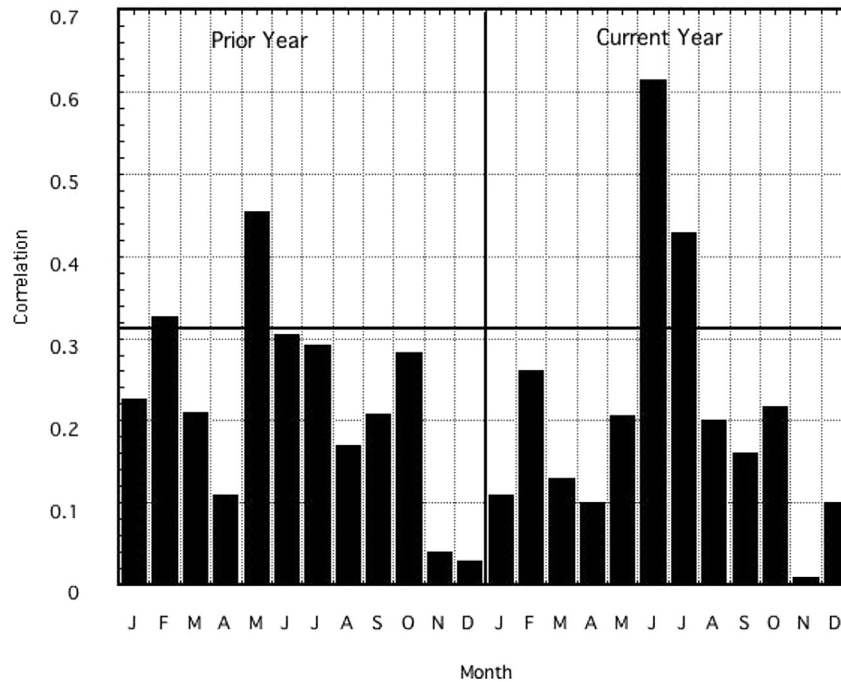


**Fig. 2.** Monthly correlation coefficients over 24 months (vertical bar shows prior year and current year) of the OZN chronology with averaged station data from four stations from Mongolia (Bulgan & Muren), and Russia (Irkutsk & Minusinsk) over the 1941–2005 common period. The Black horizontal bar signifies the 95% confidence level.

**Table 2**

Calibration and validation statistics. RE is the reduction of error, CE is coefficient of efficiency (Cook and Kairiukstis, 1990) and PR is Pearson's correlation coefficient. RE and CE are measures of shared variance between the actual and modeled series. In the calibration period, RE and CE are identical to the coefficient of determination  $R^2$ . Values above zero indicate that the regression model has skill.

	Calibration 1941–1973	Validation 1974–2005	Calibration 1974–2005	Validation 1941–1973
RE	0.340	0.456	0.551	0.327
CE	0.340	0.448	0.551	0.270
PR	0.583	0.742	0.742	0.629

(Table 3). Warmth generally persisted until nearly the end of the 1000s. This period (~900–1100) coincides with the MCA, which has been described in other proxy records for Asia (Ge and Wu, 2011; Cook et al., 2013), elsewhere across the Northern Hemisphere (Diaz et al., 2011) and the globe (Cook et al., 2002) but has been shown to vary spatially and temporally (Mann et al., 2009; PAGES 2K Consortium, 2013). 20th and 21st Century warming is higher than at any other time in the reconstruction. Mean reconstructed temperature from 990 to 1090 (the warmest part of the MCA) is 16.2 °C compared to 16.7 °C from 1905 to 2005. By comparison, average summer reconstructed temperature from 1999 to 2004 is 18.4 °C, and the 1st (1986–2005, 17.5 °C), 2nd (1941–1960, 16.9 °C) and 5th (1966–1985, 16.7 °C) warmest non-overlapping 20-year-periods occur in the 21st and 20th Century. The 3rd (996–1015, 16.9 °C) and 4th (1412–1431, 16.7 °C) warmest non-overlapping 20 year periods occurred during the MCA.

Another multi-decadal cold period began in 1111 with temperatures largely below average until 1155. 1111–1130 and 1135–1154 are the 4th and 8th coldest 20-year periods in the reconstruction, respectively. A warming trend followed and lasted nearly 300 years, peaking with warmth from 1412 to 1431 (the 4th warmest 20 year period on record) that is nearly comparable with the MCA and 20th century warming. Cold conditions are generally observed during the LIA epoch from ~1350 to 1880, particularly from 1454 to 1473 (9th coldest 20 year period), 1584–1603 (5th coldest), 1695–1714

(6th coldest), 1792–1801 (7th) and 1832–1851 (2nd). From 1832 to 1851 average summer temperatures were ~14.5 °C with cold temperatures persisting for more than two decades—from 1830 until 1854.

After the mid-1800s, cold temperatures began to warm and continued until the end of the record in 2005. Attributed to anthropogenic forcing (Masson-Delmotte et al., 2013), this warming reflects similar trends found in both recorded and paleoclimatic data from around the Northern Hemisphere (e.g. Jacoby et al., 1996; Cook et al., 2004, 2013; D'Arrigo et al., 2006; Juckes et al., 2007; PAGES 2K Consortium, 2013; Masson-Delmotte et al., 2013). In fact, seven of the ten warmest individual years and five of the warmest 20-year periods (Table 3) occur in the 20th and 21st Century. The warmest 20 year period, 1986–2005, has an average summer temperature of 17.5 °C relative to a long term mean of 15.8 °C. The 20th Century has the highest century-scale average temperatures over the length of the reconstruction, with the MCA not far behind (Table 4).

The unusually warm reconstructed temperature anomalies in the years 2003 and 2004 are consistently observed across all living tree samples as enhanced growth. There was no ecological evidence of disturbance such as logging or fire at the study site. These anomalies follow three of the warmest summers on record (2000–2002), which likely benefited radial growth as well.

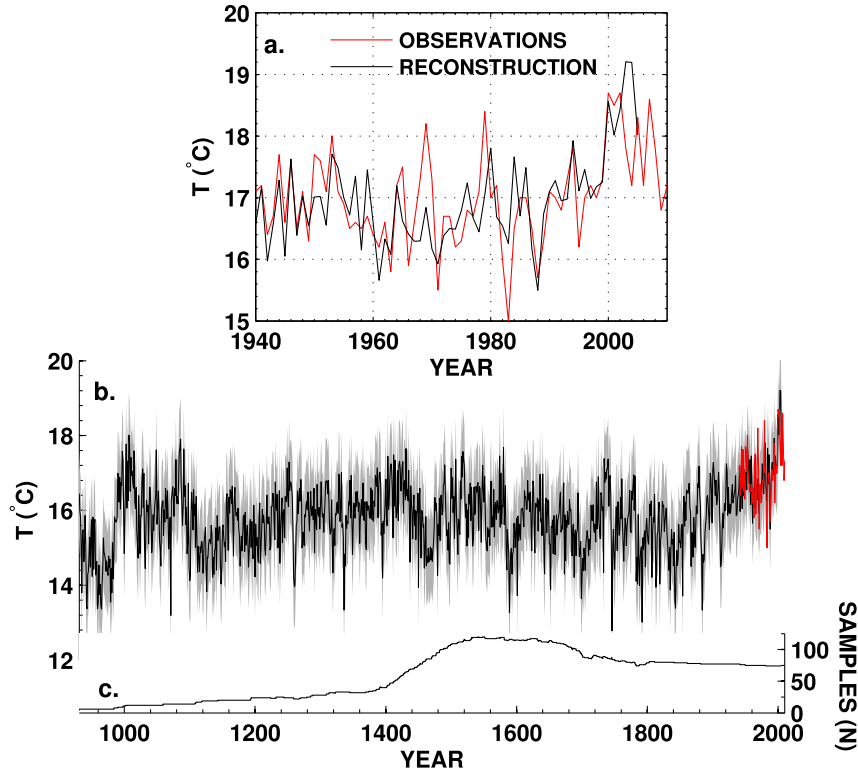


**Fig. 3.** a. Observed average June–July station temperature data (red) with the tree-ring based reconstructed data (black), and b. Northern Mongolia summer temperature reconstruction spanning 931–2005 with sample depth. The observed record is in red and error envelope on panel b is plus/minus 2 root mean square error. (For interpretation of the references to colour in this figure legend, the reader is referred to the web version of this article.)

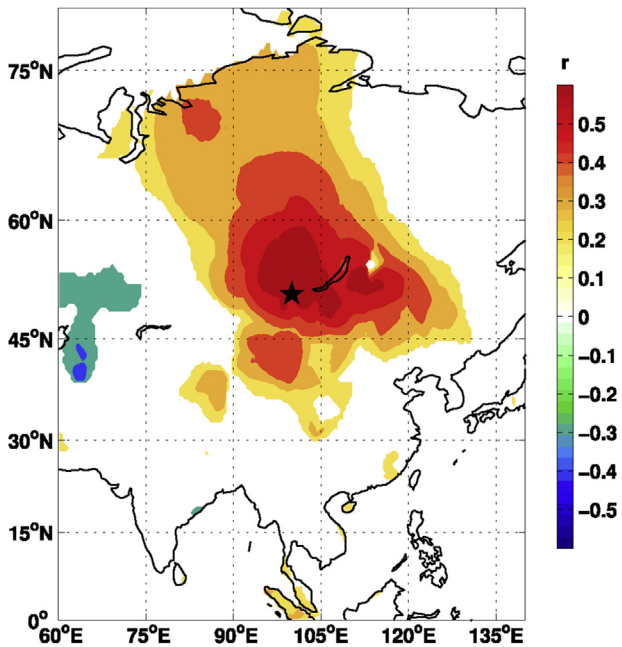


**Fig. 4.** Spatial correlation map of the OZN chronology with CRUTS3.10 average June–July temperatures from 1941 to 2005. The linear trend was determined and subtracted from all data prior to correlating variables. For grid point data, the linear trend is subtracted from each grid point individually from all data. A similar but weaker pattern emerges using CRU data from 1901 to 1940 (not shown), however the underlying data is sparse. The OZN site location is marked by a star.

**Table 3**  
Warmest/coldest non-overlapping period table.

	1-yr	3-yr	20-yr
<b>A. Warmest</b>			
1	2003	2002–2004	1986–2005
2	2004	1999–2001	1941–1960
3	2000	1084–1086	996–1015
4	2002	1994–1996	1412–1431
5	2005	1007–1009	1966–1985
6	2001	1953–1955	1074–1093
7	1007	1518–1520	1891–1910
8	1994	1984–1986	1725–1744
9	1086	1420–1422	1921–1940
10	1008	1738–1740	1511–1520
<b>B. Coldest</b>			
1	1746	963–965	956–975
2	1792	942–944	1832–1851
3	1071	1842–1844	932–953
4	1589	959–961	1111–1130
5	1336	979–981	1584–1603
6	1884	1259–1261	1695–1714
7	965	1589–1591	1792–1801
8	943	1699–1701	1135–1154
9	959	1336–1338	1454–1473
10	1843	1884–1886	1186–1205

4.2. Comparison to other records

There are relatively few tree-ring proxy records for temperature in Mongolia. Four temperature-sensitive alpine tree-line records were produced by D'Arrigo et al. (2000) that dated back to 1450 and reflected regional and Northern Hemisphere scale temperature variations. Of those, one site (Sol Dav) was revisited to sample 'relict' wood that resulted in a temperature sensitive chronology

**Table 4**  
Century-scale average temperature in °C.

931–999	15.02
1000–1099	16.14
1100–1199	15.32
1200–1299	15.78
1300–1399	15.96
1400–1499	15.95
1500–1599	15.94
1600–1699	15.66
1700–1799	15.57
1800–1899	15.57
1900–1999	16.60

dating back to 262CE (D'Arrigo et al., 2001a). More recently, a large network of tree-ring chronologies was used to reconstruct summer temperature for temperate East Asia, north of 23°N (Pages 2K Consortium, 2013; Cook et al., 2013) from 800 to 1989. The four chronologies from D'Arrigo et al. (2000 and 2001a) were used as part of that large-scale reconstruction along with 418 other chronologies as potential predictors.

The OZN and Sol Dav records correlate significantly ( $r = 0.5$ ,  $p < 0.05$ ) over the 900–1999 common period and all three reconstructions have good agreement prior to the late 1300s (Fig. 5). The OZN reconstruction shows that the warm early MCA occurred from ~990 to 1110 in Northern Mongolia. This MCA warm period is consistent with the Pages Asia 2K record, but not the Sol Dav record (WI- Fig. 5). Sol Dav shows considerably more warming (inferred) beginning in the 900s. The period from ~1110 to 1160 is a very cold period for Sol Dav, OZN, and Asia 2K (CI – Fig. 5) and is followed by a general warming trend in OZN that peaks in the early 1400s that is seen in all three records (WII- Fig. 5). Very cold temperatures occur in all three records from the 1450s to the 1470s (CII- Fig. 5), and again from the late 1500s to the early 1600s (CIII- Fig. 5). During the 19th century, all records show cooling in the mid 1800s (CIV- Fig. 5). Sol Dav has much less growth (inferred cooling) than OZN

from ~1800 to 1910. A warming trend consistent with global temperature patterns begins in the 1850 s at OZN, 1870 s at Sol Dav and 1880s in the Pages Asia2K reconstruction and continues for the remainder of the record (WIII- Fig. 5). Since 1999, to the end of the OZN tree-ring reconstruction in 2005, summer warmth exceeds warmth seen at any other time. At Sol Dav, increased growth (inferred warming) that exceeds any other time begins in the 1960s. The differences in Sol Dav and OZN persist even when the chronologies are standardized in the same manner.

#### 4.3. Volcanic influence on Mongolian climate

Cooling associated with explosive volcanic eruptions can influence tree growth and provides one line of evidence for the timing and magnitude of such events and their influence on the climate system (Jones et al., 1995; Briffa et al., 1998; D'Arrigo and Jacoby, 1999, 2013). Ring width can be a useful parameter for volcano-climate studies, although maximum latewood density, due to its considerable sensitivity to such events, is generally considered more appropriate for quantitative evaluations of past volcanism (D'Arrigo et al., 2013). The formation of frost-rings, rings that have damaged and resinous cells due to sudden volcanic cooling, and light-rings have been closely linked with the occurrence of major volcanic eruptions (Lamarche and Hirschboeck, 1984; Fillon et al., 1986; Yamaguchi et al., 1993; D'Arrigo et al., 2003; Hantemirov et al., 2004). At OZN we observe evidence of significant volcanic influence manifested as narrow rings, micro-rings (barely visible rings that are only a few cells wide), and missing rings that coincide with known eruptions. The years 934 (below average) and 935 (-2 standard deviations (SD)), the first two years of the 900s multi-decadal cold period (934–984), coincide with a massive eruption at Eldgja, Iceland (Volcanic Explosivity Index (VEI) = 6), Simkin and Siebert 1994; Stothers et al., 1998), which may have affected temperatures for up to 8 years after the event (D'Arrigo et al., 2001b). At Sol Dav (262–1999 C.E.), the year 935 was slightly below average

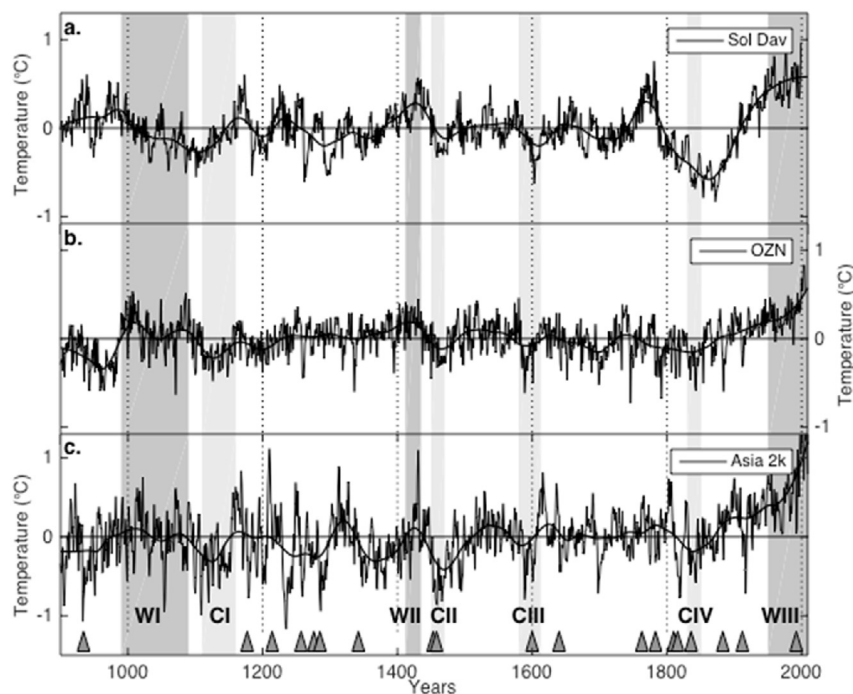


**Fig. 5.** A comparison of Sol Dav (a.), the OZN reconstruction (b.), and the Asia 2K reconstruction (c.). CI to CV refers to cold periods, and WI to WIII to warm periods, which are consistent in all reconstructions. The y-axis for OZN is on the right, Sol Dav & Asia 2k on the left. Triangles signify volcanic years.

and frost rings were observed in the early wood during the year 938. No evidence of frost damage is found in the OZN cores or sections, although larch may be a more resistant species to frost damage than pine (Voskela, 1970). A micro-ring occurs in year 1177 (-2SD) and may be a result of Haku-San, in Honshu, Japan (VEI = 3) and Katla in Iceland (VEI = 2, Simkin and Siebert, 1994), although the exact date of these eruptions and their climatic impact are not accurately known. Another significant event, now believed to be the eruption of Samalas (Indonesia) occurred in 1257 (Lavigne et al., 2013). The trees at the OZN site formed micro-rings in 1258 and for 4 years after the event; 1258 (-1SD), 1259 (-2SD), 1260 (-2SD), 1261 (-2SD), and 1262 (-1SD), with one core missing a ring in 1259. This volcanic signal was also detected in the Sol Dav chronology; ring width was average in 1258, and below average from 1261 until 1268, with a growth low at 1262 (-2SD).

Several large-scale tropical volcanic events occurred during the LIA and are evident in the rings from the OZN site. The early 1450s eruption, believed to be in 1453 or 1454 from Kuwae in Vanuatu (Briffa et al., 1998; Gao et al., 2006), although now uncertain (Cole-Dai et al., 2013; Sigl et al., 2014), manifests as a slightly narrow ring at 1453 and a micro-ring (-1SD) in 1454. We also find a micro ring at 1458 (-1SD), which Plummer et al. (2012) suggest could be from Kuwae, based on the size and shape of the caldera and the eruption characteristics, however they urge caution in assigning the eruptions of the 1450s to a particular source. The 1600 eruption at Huaynaputina in Peru (VEI = 6, Briffa et al., 1998) manifested as a micro-ring in 1601 (nearly -3SD) and two cores with missing rings. Micro-rings were found from 1601 to 1604 with the

narrowest being 1603 (-3SD) and 1604 (-1SD) at Sol Dav. Narrow rings and micro-rings were found in the OZN site at 1642 (-1SD) and 1643 (-2SD), and from 1641 to 1644 at Sol Dav, that coincide with the 1640 eruption of Komaga-Take, in Japan (VEI 5). Briffa et al. (1998) suggested that the 1640 eruption of Parker volcano in Philippines (VEI = 6) might have also contributed to the cold summer temperature anomalies observed in 1641. The 1783 (-1SD) Laki eruption (VEI = 6) appears to have resulted in a 2° summer cooling and missing rings in 11 out of the 75 samples that cover that time period. The eruption of 1883 in Krakatoa, Indonesia (VEI = 6, Briffa et al., 1998) manifested as a micro-ring in 1884 (nearly -3 SD) with 22 cores out of 77 missing a ring for that year. No evidence of frost rings or damage to the cells was evident in the OZN samples and Sol Dav shows only narrow ring in 1884. Narrow rings and were also found at 1912 (-2SD), 1913, (-2SD) and 1914 (-1SD) that coincide with the 1912 Katmai (VEI = 6) eruption with summer temperatures 1° colder during 1912 than during the previous summer.

Superposed Epoch Analysis provides additional support for these observations. Based on events defined using the data from Crowley et al. (2008), cooling occurred during the year of the event as well as the following year, with five subsequent years of colder temperatures (Fig. 6 a & c). Based on the Gao et al. (2008) event list there is significant cooling the year of the event followed by one additional significant year of cooling (Fig. 6 b & d). The shift between maximum observed cooling in Year 0 (the event year) vs Year 1 is attributable to the differences in the forcing datasets (Schmidt et al., 2012) for the maximum negative radiative forcing

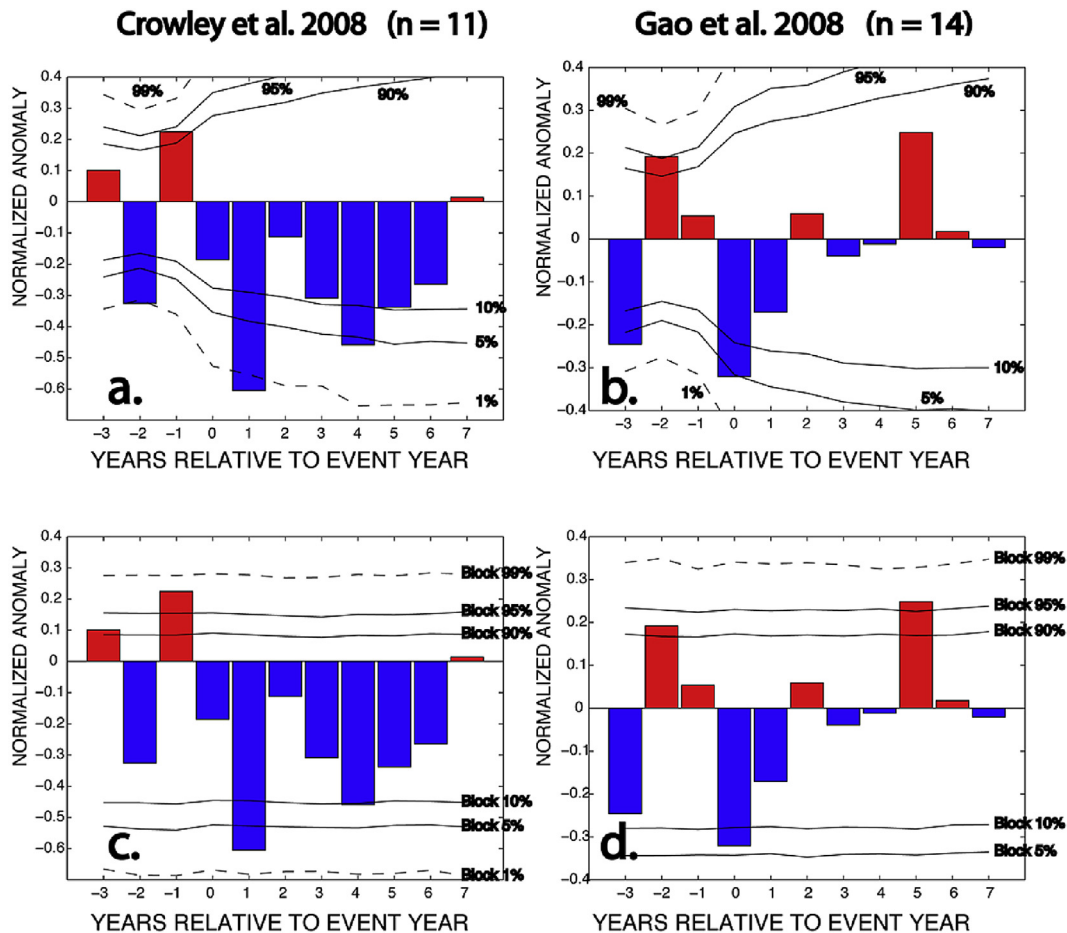


Fig. 6. Results of the superposed epoch analysis (SEA) using two types of significance tests; random sampling (a & b) and block reshuffling (c & d).

years, e.g. 1258 vs 1259, 1641 vs 1642, 1815 vs 1816. This observation emphasizes the importance of considering uncertainty in the forcing data (Schmidt et al., 2012; Sigl et al., 2014) when evaluating the impact of volcanic eruptions on climate using proxy records (Anchukaitis et al., 2012; D'Arrigo et al., 2013).

#### 4.4. Human impacts

The OZN site used in the reconstruction here is relatively mesic, and therefore, these trees, have been immune from drought stress during periods of enhanced temperatures. However, temperature increases in recent years could have contributed to moisture deficits in many other regions of Mongolia; the summer temperatures between 1999 and 2002 observed in our reconstruction as a period of anomalously high temperatures could have exacerbated one of the worst droughts of the past four centuries across Mongolia (Davi et al., 2010) or past millennium in central Mongolia (Pederson et al., 2014). This drought, by means of affecting available forage resources, was also one of the contributing factors to the mass mortality of livestock seen in those years (Sheffield and Wood, 2012). Recent drought conditions in Mongolia are associated with increased grassland fires (Farukh et al., 2009), which act in conjunction with modern pressures like grassland degradation from increasing goat populations, and have resulted in the expansion of desert areas from the dry and arid southern Mongolia towards central and northern regions of the country (Liu et al., 2013). Therefore, while the trees in our study site may have benefitted from the recent warming, the deleterious impact of this temperature increase was much more widespread. Though increases in precipitation are projected in Mongolia over the next century (Masson-Delmotte et al., 2013), warmer temperatures could increase evaporative demand (Sato et al., 2007; Cook et al., 2014). This effect could be detrimental to this semi-arid region in the future, which relies heavily on its agricultural economic sector.

## 5. Conclusion

Millennial-length tree-ring chronologies that are sensitive to temperature variations are extremely limited in Central Asia. We have described a well-calibrated and verified millennial-length tree-ring reconstruction of summer temperatures from Mongolia and vicinity—the second millennial length, alpine tree-line temperature sensitive chronology from Mongolia. This reconstruction puts an unusual and unprecedented recent warming trend (since ~ the 1990s) into a long-term context and allows for evaluation of the spatial and temporal variations of the MCA and LIA across Asia. This reconstruction also allows for evaluation of volcanic influence on Mongolian and Central Asian climate.

## Acknowledgements

In memory of Dr. Gordon C. Jacoby. This research was supported by the National Science Foundation under grants AGS-PRF #1137729, ATM0117442, and AGS0402474. We thank Dr. Markus Stoffel, and an anonymous reviewer for their insightful comments. We also thank the Global Historical Climatology Network of NCDC/NOAA, Goddard Institute of Space Studies, and the Climate Research Unit for meteorological data used in this study and Dr. van Oldenborgh for maintaining KNMI Climate Explorer. Field sampling was aided by students and staff of the Tree-Ring Laboratory of the Dept. of Forestry, Faculty of Biology, National University of Mongolia; and with the cooperation of the Mongolian Ministry of Nature and Environment. Lamont-Doherty Earth Observatory publication no, 7900.

## References

- Adams, J.B., Mann, M.E., Ammann, C.M., 2003. Proxy evidence for an El Niño-like response to volcanic forcing. *Nature* 426, 274–278.
- Anchukaitis, K.J., Breitenmoser, P., Briffa, K.R., Buchwal, A., Buntgen, U., Cook, E.R., D'Arrigo, R.D., Esper, J., Evans, M.N., Frank, D., Grudd, H., Gunnarson, B., Hughes, M.K., Kirdyanov, A.V., Korner, C., Krusic, P., Luckman, B., Melvin, T.M., Salzer, M.W., Shashkin, A.V., Timmreck, C., Vaganov, E.A., Wilson, R., 2012. Tree rings and volcanic cooling. *Nat. Geosci.* 5, 836–837.
- Briffa, K., Jones, P., Schweingruber, F., Osborn, T., 1998. Influence of volcanic eruption on Northern Hemisphere temperature over the past 600 years. *Nature* 391, 678–682.
- Chen, F., Wang, J., Jin, L., Zhang, Q., Li, J., Chen, J., 2009. Rapid warming in mid-latitude central Asia for the past 100 years. *Front. Earth Sci. China* 3 (1), 42–50.
- Cole-Dai, J., Ferris, D.G., Lanciki, A.L., Savarino, J., Thieme, M.H., McConnell, J.R., 2013. Two likely stratospheric volcanic eruptions in the 1450s C.E. found in a bipolar, subannually dated 800 year ice core record. *J. Geophys. Res. Atmos.* 118, 7459–7466.
- Cook, B.L., Smerdon, J.E., Seager, R., Coats, S., 2014. Global warming and 21st century drying. *Clim. Dyn.* 43, 2607–2627.
- Cook, E.R., Kairiukstis, L.A., 1990. *Methods of Dendrochronology, Applications in the Environmental Sciences*. Kluwer Academic Press, Dordrecht, p. 394.
- Cook, E.R., Briffa, K., Jones, P., 1994. Spatial regression methods in dendroclimatology: a review and comparison of two techniques. *Int. J. Climatol.* 14 (4), 379–402.
- Cook, E.R., Briffa, K.R., Meko, D.M., Graybill, D.A., Funkhouser, G., 1995. The segment length curve in long tree-ring chronology development for paleoclimatic studies. *Holocene* 5, 229–237.
- Cook, E.R., Peters, K., 1997. Calculating unbiased tree-ring indices for the study of climatic and environmental change. *Holocene* 7 (3), 359–368.
- Cook, E.R., Esper, J., D'Arrigo, R., 2004. Extra-tropical Northern Hemisphere land temperature variability over the past 1000 years. *Quat. Sci. Rev.* 23, 2063–2074.
- Cook, E.R., Palmer, J., D'Arrigo, R., 2002. Evidence for a 'Medieval Warm Period' in a 1,100 year tree-ring reconstruction of past austral summer temperatures in New Zealand. *Geophys. Res. Lett.* 29 (14), 12 1–12 4.
- Cook, E.R., Krusic, P., Anchukaitis, K., Buckley, B., Nakatsuka, T., Sano, M., PAGES Asia2K Members, 2013. Tree-ring reconstructed summer temperature anomalies for temperate East Asia since 800 C.E. *Clim. Dyn.* 41, 2957–2972.
- Crowley, T.J., Zielinski, G., Vinther, B., Udisti, R., Kreutz, K., Cole-Dai, J., Castellano, E., 2008. Volcanism and the Little Ice Age. *PAGES Newsl.* 16, 22–23.
- D'Arrigo, R., Jacoby, G., 1999. Northern North American tree-ring evidence for regional temperature changes after major volcanic events. *Clim. Change* 41, 1–15.
- D'Arrigo, R., Jacoby, G., Pederson, N., Frank, D., Buckley, B., Nachin, B., Mijiddorj, R., Dugarjav, C., 2000. Mongolian tree-rings, temperature sensitivity and reconstructions of Northern Hemisphere temperature. *Holocene* 10 (6), 669–672.
- D'Arrigo, R., Jacoby, G., Frank, D., Pederson, N., Cook, E., Buckley, B., Nachin, B., Mijiddorj, R., Dugarjav, C., 2001a. 1738 years of Mongolian temperature variability inferred from a tree-ring record of Siberian pine. *Geophys. Res. Lett.* 28, 543–546.
- D'Arrigo, R., Frank, D., Jacoby, G., Pederson, N., 2001b. Spatial response to major volcanic events in or about AD 536, 934 and 1258: frost rings and other dendrochronological evidence from Mongolia and northern Siberia: comment on R. B. Stothers, 'volcanic dry fogs, climate cooling, and plague pandemics in Europe and the middle east'. *Clim. Change* 49, 239–246.
- D'Arrigo, R., Frank, D., Jacoby, G., Pederson, N., 2003. Spatial response to major volcanic events in or about AD 536, 934 and 1258: frost rings and other dendrochronological evidence from Mongolia and northern Siberia. In: Robock, A., Oppenheimer, C. (Eds.), *Volcanism and Earth's Atmosphere*. AGU, Washington D. C., pp. 255–261.
- D'Arrigo, R., Wilson, R., Jacoby, J., 2006. On the long-term context for late twentieth century warming. *J. Geophys. Res. – Atmos.* 111 (D03103), 1–12.
- D'Arrigo, R., Wilson, R., Anchukaitis, K.J., 2013. Volcanic cooling signal in tree ring temperature records for the past millennium. *J. Geophys. Res. Atmos.* 118 (16), 9000–9010.
- Davi, N., Jacoby, G., Fang, K., Li, J., D'Arrigo, R., Baatarbileg, N., Robinson, D., 2010. Reconstructed drought across Mongolia based on a large-scale tree-ring network: 1520–1993. *J. Geophys. Res.* 115 (D22103), 1–9.
- Diaz, H.F., Trig, R., Hughes, M.K., Mann, M.E., Xoplaki, E., Barriopedro, D., 2011. Spatial and temporal characteristics of climate in Medieval Times revisited. *Bull. Am. Meteorol. Soc.* 1487–1500. November.
- Farukh, M.A., Hayasaka, H., Mishigdorj, O., 2009. Recent tendency of Mongolian woodland fire incidence: analysis using MODIS hotspot and weather data. *J. Nat. Disaster Sci.* 31 (1), 23–33.
- Filion, L., Payette, S., Gauthier, L., Boutin, Y., 1986. Light rings in subarctic conifers as a dendrochronological tool. *Quat. Res.* 26, 272–279.
- Fischer, E.M., Luterbacher, J., Zorita, E., Tett, S.F.B., Casty, C., Wanner, H., 2007. European climate response to tropical volcanic eruptions over the last half millennium. *Geophys. Res. Lett.* 34 (5), L05707.
- Gao, C., Robock, A., Self, S., Witter, J.B., Steffenson, J.P., Clausen, H.B., Siggaard-Andersen, M.-L., Johnsen, S., Mayewski, P.A., Ammann, C., 2006. The 1452 or 1453 A.D. Kuwae eruption signal derived from multiple ice core records: greatest volcanic sulfate event of the past 700 years. *J. Geophys. Res.* 111 (D12), 1–11.



- Gao, C.C., Robock, A., Ammann, C., 2008. Volcanic forcing of climate over the past 1500 years: an improved ice core based index for climate models. *J. Geophys. Res.* 113 (D23111), 1–15.
- Ge, Q., Wu, W., 2011. Climate during the MCA in China. In: Xoplaki, E., Fleitmann, D., Diaz, H., von Gunten, L., Kiefer, T. (Eds.), *PAGES News*, 19, 1.
- Hantemirov, R.M., Gorlanova, L.A., Shiyatov, S.G., 2004. Extreme temperature events in summer in northwest Siberia since AD 742 inferred from tree rings. *Paleogeogr. Paleoclimatol. Paleoecol.* 209, 155–164.
- Harris, I., Jones, P.D., Osborn, T.J., Lister, D.H., 2014. Updated high-resolution grids of monthly climatic observations. *Int. J. Climatol.* 34 (3), 623–642.
- Haurwitz, M.W., Brier, G.W., 1981. A critique of the superposed epoch analysis method—its application to solar-weather relations. *Mon. Weather Rev.* 109 (10), 2074–2079.
- Jacoby, G., D'Arrigo, R., Davaajamts, T., 1996. Mongolian tree rings and 20th century warming. *Science* 273, 771–773.
- Jones, P., Briffa, K., Scheingruber, F., 1995. Tree-ring evidence of the widespread effects of explosive volcanic eruptions. *Geophys. Res. Lett.* 22 (11), 1333–1336.
- Juckes, M.N., Allen, M.R., Briffa, K.R., Esper, J., Hegerl, G.C., Moberg, A., Osborn, T.J., Weber, S.L., 2007. Millennial temperature reconstruction intercomparison and evaluation. *Clim. Past.* 3, 591–609.
- Lamarque, V.C., Hirschboeck, K.K., 1984. Frost rings in trees as records of major volcanic eruptions. *Nature* 307, 121–126.
- Lamb, H.H., 1965. The early medieval warm epoch and its sequel. *Palaeogeogr. Palaeoclimatol. Paleoecol.* 1, 13–37.
- Lavigne, F., Degeai, J.P., Komorowski, J.C., Guillet, S., Robert, V., Lahitte, P., Oppenheimer, C., Stoffel, M., Vidal, C.M., Surono, Pratomo, I., Wassmer, P., Hajdas, I., Sri Hadmoko, D., de Belizal, E., 2013. Source of the great A.D. 1257 mystery eruption unveiled, Samalas volcano, Rinjani Volcanic Complex, Indonesia. *PNAS* 110 (42), 16742–16747.
- Liu, Y.Y., Evans, J.P., McCabe, M.F., de Jeu, R.A., van Dijk, A.I., Dolman, A.J., Saizen, I., 2013. Changing climate and overgrazing are decimating Mongolian steppes. *PLoS One* 8 (2), e57599. <http://dx.doi.org/10.1371/journal.pone.0057599>.
- Mann, M.E., Zhang, Z., Rutherford, S., Bradley, R.S., Hughes, M.K., Shindell, D., Ammann, C., Faluvegi, G., Ni, F., 2009. Global signatures and dynamical origins of the little ice age and medieval climate anomaly. *Science* 326 (5957), 1256–1260.
- Masson-Delmotte, V., Schulz, M., Abe-Ouchi, A., Beer, J., Ganopolski, A., González Rouco, J., Jansen, E., Lambeck, K., Luterbacher, J., Naish, T., Osborn, T., Otto-Bliesner, B., Quinn, T., Ramesh, R., Rojas, M., Shao, X., Timmermann, A., 2013. Information from paleoclimate archives. In: Stocker, T., Qin, D., Plattner, G.K., Tignor, M., Allen, S., Boschung, J., Nauels, A., Xia, Y., Bex, V., Midgley, R. (Eds.), *Climate Change 2013. The Physical Science Basis. Contribution of Working Group I to the Fifth Assessment Report of the Intergovernmental Panel on Climate Change*. Cambridge University Press, Cambridge, United Kingdom and New York, NY, USA, pp. 383–464.
- Melvin, T.M., Briffa, K.R., Nicolussi, K., Grabner, M., 2007. Time-varying-response smoothing. *Dendrochronologia* 25, 65–69.
- Melvin, T.M., Briffa, K.R., 2008. A “signal-free” approach to dendroclimatic standardization. *Dendrochronologia* 26, 71–86.
- Melvin, T.M., Briffa, K.R., 2013. CRUST: software for the implementation of regional chronology standardization: Part 1. Signal-Free RCS. *Dendrochronologia* 32, 7–20.
- Mygland, V., Zharnikova, O.A., Malysheva, N.V., Gerasimova, O.V., Vaganov, E.A., Sidorova, O.V., 2012. Constructing the tree-ring chronology and reconstructing summertime air temperatures in southern Altai for the last 1500 years. *Geogr. Nat. Resour.* 33, 200–207.
- PAGES 2K Consortium, 2013. Continental-scale temperature variability during the past two millennia. *Nat. Geosci.* 6, 339–346.
- Pederson, N., Hessel, A.E., Baatarbileg, N., Anchukaitis, K.J., Di Cosmo, N., 2014. Pluvials, droughts, the Mongol Empire, and modern Mongolia. *Proc. Natl. Acad. Sci.* 111 (12), 4375–4379.
- Plummer, C.T., Curran, M.A.J., van Ommen, T.D., Rasmussen, S.O., Moy, A.D., Vance, T.R., Clausen, H.B., Vinther, B.M., Mayewski, P.A., 2012. An independently dated 2000-yr volcanic record from Law Dome, East Antarctica, including a new perspective on the dating of the 1450s CE eruption of Kuwae, Vanuatu. *Clim. Past.* 8, 1929–1940.
- Sato, T., Kimura, F., Kitoh, A., 2007. Projection of global warming onto regional precipitation over Mongolia using a regional climate model. *J. Hydrol.* 333, 144–154.
- Schmidt, A., Carslaw, K.S., Mann, G.W., Rap, A., Pringle, K.J., Spracklen, D.V., Wilson, M., Forster, P.M., 2012. Importance of tropospheric volcanic aerosol for indirect radiative forcing of climate. *Atmos. Chem. Phys.* 12, 7321–7339.
- Sheffield, J., Wood, E.F., 2012. *Drought: Past Problems and Future Scenarios*. Earthscan, London, 2011.
- Sigl, M., McConnell, J.R., Toohey, M., Curran, M., Das, S., Edwards, R., Isaksson, E., Kawamura, K., Kipfstuhl, S., Krüger, K., Layman, L., Maselli, O., Motizuki, Y., Motoyama, H., Pasteris, D., Severi, M., 2014. Insights from Antarctica on volcanic forcing during the Common Era. *Nat. Clim. Change* 4, 693–697.
- Simkin, T., Siebert, L., 1994. *Volcanoes of the World*, second ed. Geoscience Press, Tucson.
- Stothers, R., 1998. Far reach of the tenth century Eldgja eruption, Iceland. *Clim. Change* 39, 715–726.
- Voskela, V., 1970. Frost damage on Norway Spruce, Scots Pine, Silver Birch and Siberian Larch in the forest fertilizer experimental area at Kivisuo. *Folia Inst. For. Fenn.* 78, 25.
- Wigley, T.M.L., Briffa, K.R., Jones, P.D., 1984. On the average value of correlated time series, with applications in dendroclimatology and hydrometeorology. *J. Appl. Meteorol.* 23, 201–213.
- Yamaguchi, D.K., Filion, L., Savage, M., 1993. Relationship of temperature and light ring formation at subarctic tree line and implications for climate reconstruction. *Quat. Res.* 39, 256–262.